Environ Geochem Health
https://doi.org/10.1007/s10653-020-00614-2

ORIGINAL PAPER

Spatial distribution, risk assessment, and source identification of heavy metals in water from the Xiangxi River, Three Gorges Reservoir Region, China

Biao Xiong · Ruiping Li · David Johnson · Yuhong Luo · Ying Xi · Dong Ren · Yingping Huang

Received: 25 May 2019 / Accepted: 4 June 2020

Abstract Heavy metals (HMs) contamination in rivers has attracted wide concern due to its persistence and potential risks to the natural environment and human health. In this study, eight HMs (As, Hg, Cu, Pb, Ca, Zn, Mn, and Ni) were measured by inductively coupled plasma mass spectrometry in 24 water samples to investigate HMs contamination levels in the Xiangxi River of the Yangtze River basin. A geographic information systems kriging interpolation method was used to reveal the spatial distribution of HMs contamination. The results indicate that most HMs occurred at acceptable levels below the Surface Water Quality Standard (GB 3838-2002), with the highest concentration (23.23 mg kg^{-1}) of Mn being observed at sampling site X20. The values of the potential ecological risk index (RI) suggest that high potential ecological risks were present at sampling sites X1, X3, X4, X14, X16, X17, and X24, which reached moderate risk level. The highest value of RI (279.56) was observed at site X17. HM spatial distributions show that upstream pollution is more severe than downstream. The hazard index was below 1 for all HMs except for Mn, indicating that HMs in Xiangxi River pose a low risk to human health. HM source identification was accomplished using principal component analysis and Pearson's correlation. Cu, Cd, Ni, and Hg originate primarily from agriculture, while Pb, Zn, and As originate primarily from transportation and mining. This research provides a reference on the risks posed by HMs in Xiangxi River and will support efforts to protect and improve water quality in Xiangxi River.

Keywords Heavy metal · Xiangxi River · Spatial distribution · Risk assessment

Electronic supplementary material The online version of this article (https://doi.org/10.1007/s10653-020-00614-2) contains supplementary material, which is available to authorized users.

B. Xiong · R. Li (✉) · Y. Luo · Y. Xi · Y. Huang
College of Hydraulic and Environmental Engineering, China Three Gorges University, Yichang 443002, Hubei, China

B. Xiong · R. Li · Y. Luo · Y. Xi · D. Ren · Y. Huang
Hubei Engineering Technology Research Center for Farmland Environment Monitoring, China Three Gorges University, Yichang 443002, Hubei, China

B. Xiong · R. Li · D. Johnson · Y. Luo · Y. Xi · D. Ren · Y. Huang (✉)
Engineering Research Center of Eco-Environment in Three Gorges Reservoir Region of Ministry of Education, China Three Gorges University, Yichang 443002, Hubei, China
e-mail: chem_ctgu@126.com

Introduction

HMs have strong geochemical activity and can easily migrate in water, suspended particulate, and sediments (Zhuang et al. 2018). Though most HMs exhibit strong

Published online: 13 June 2020

biological activity and are resistant to biodegradation, they can accumulate through the food chain and end up in the human body (Zhang et al. 2019). When their concentration in the human body exceeds a particular safety threshold, HMs can exhibit deleterious properties such as carcinogenicity, teratogenicity, and mutagenicity (Rehman et al. 2018). For example, excessive Pb concentrations can affect human intelligence (Lazo et al. 2018), whereas excessive amounts of Cd can have skeletal and hepatic consequences and increase the risk of lung cancer (Liu et al. 2018a). Zhu et al. (2019) analyzed six HMs (Cd, Cr, Cu, Ni, Pb, and Zn) in sediment from Fuling to Zigui in the mainstream of TGR to assess the contamination and ecological risk in this area. The results showed that the study area was contaminated by Cd, Cu, and Pb, which may have originated from agricultural fertilizer, the mining industry, and fuel combustion. Furthermore, Zhang et al. (2017a) determined the HMs content in the sediment of the Pearl River Estuary (PRE) and assessed the degree of HMs contamination using the geoaccumulation index method. The results indicated that the levels of HMs had strongly increased.

The Three Gorges Reservoir (TGR), located in the upper reaches of the Yangtze River, is the world's largest hydroelectric facility and provides important benefits include flood control, power generation, navigation, etc. (Huang et al. 2019). The TGR is an anti-seasonal and periodic impoundment operation, with a high water level (175 m) in winter (dry season) and a low level (145 m) in summer (wet season). This annual operating cycle provides irrigation water in the dry season and enhanced flood control in the wet season (Lin et al. 2018; Wu et al. 2016). After the impoundment operation of the TGR, the concentrations of the heavy metals (HMs) As, Cd, Cr, Cu, Ni, Pb, Zn, and especially Hg, increased in the TGR mainstream and approached the threshold value (Zhao et al. 2017). Moreover, previous studies have identified that rapid economic development has increased the discharge of sewage from chemical enterprises, automobile exhaust emissions, and the use of agricultural fertilizers and pesticides, which together have increased the concentration of HMs in water environments over time (Bai et al. 2019).

Xiangxi River is the largest tributary to the lower TGR, flowing into TGR 34.5 km above the dam with a drainage area of 3099.4 km^2. It is also the tributary greatly affected by impoundment of water in TGR (Yan et al. 2016). Since 2008, HMs may move into Xiangxi River when water in the mainstream of the TGR backflowed into the river during the water impoundment period (Chuo et al. 2019). Thus, the flow regulation by the TGR may affect the concentration and distribution of HMs in the water of the Xiangxi River and may pose a potential ecological risk and health threat to the residents who live around the river. Moreover, the area around the Xiangxi River is characterized by widespread agricultural development, dense population, multiple phosphate mines, and busy roads (Yan et al. 2016), which are all potential sources of HMs pollution.

The water quality in the Xiangxi River has a great influence on the whole TGR area. Therefore, the surface water quality in the Xiangxi River has attracted a large amount of research attention by domestic and international scholars (Gao et al. 2016). Although some researchers have explored the contamination of HMs in the mainstream of the TGR, few reports exist of the concentrations of HMs in Xiangxi River (Lin et al. 2020). Previous research on the HMs content of the Xiangxi River has focused on the transfer and transformation of HMs in the soil along the hydro-fluctuation belt and the reservoir bank (Xu et al. 2014). HMs concentrations and the morphology of HMs in sediments change after flooding (Wang et al. 2017). However, the concentration of HMs in surface water of the Xiangxi River, the spatial distribution of HMs along the Xiangxi River, the potential ecological risk of HMs, and the sources of HMs have been less studied, and such data are urgently needed to support pollution prevention and environmental protection in the TGR. Therefore, it is of great significance to evaluate the degree of HMs pollution in water environments around the TGR.

This paper reports the first comprehensive investigation to evaluate the concentration of HMs (As, Hg, Cu, Pb, Ca, Zn, Mn, and Ni) in the Xiangxi River. This study had three main purposes: (1) investigate HMs contamination in the Xiangxi River and characterize its spatial distribution; (2) evaluate the ecological risks and health risks which this HMs contamination poses to local residents; and (3) identify the possible sources of this HMs contamination.

Materials and methods

Study area

Xiangxi River is a tributary of Yangtze River, located 40 km upstream of the dam (Fig. 1). Originating in Shennongjia in northwest Hubei Province, Xiangxi River is 97.3 km long, with a basin area of 3099.4 km^2 (Gao et al. 2018b; Yan et al. 2016). The average flow of the Xiangxi River basin is about 40.18 m^3/s, and the basin is rich in phosphorus resources. The main type of transportation on the river is shipping (Liu et al. 2017).

The Xiangxi River flows through Xingshan and Zigui County from north to south and ultimately flows into the Yangtze River. Both sides of the Xiangxi River basin are largely covered by vegetation, with a forest coverage rate of 70.9%, a farmland coverage rate of 6.5%, a water resource coverage rate of 5.3%, and a wasteland coverage rate of 4.4% (Luo et al. 2016).

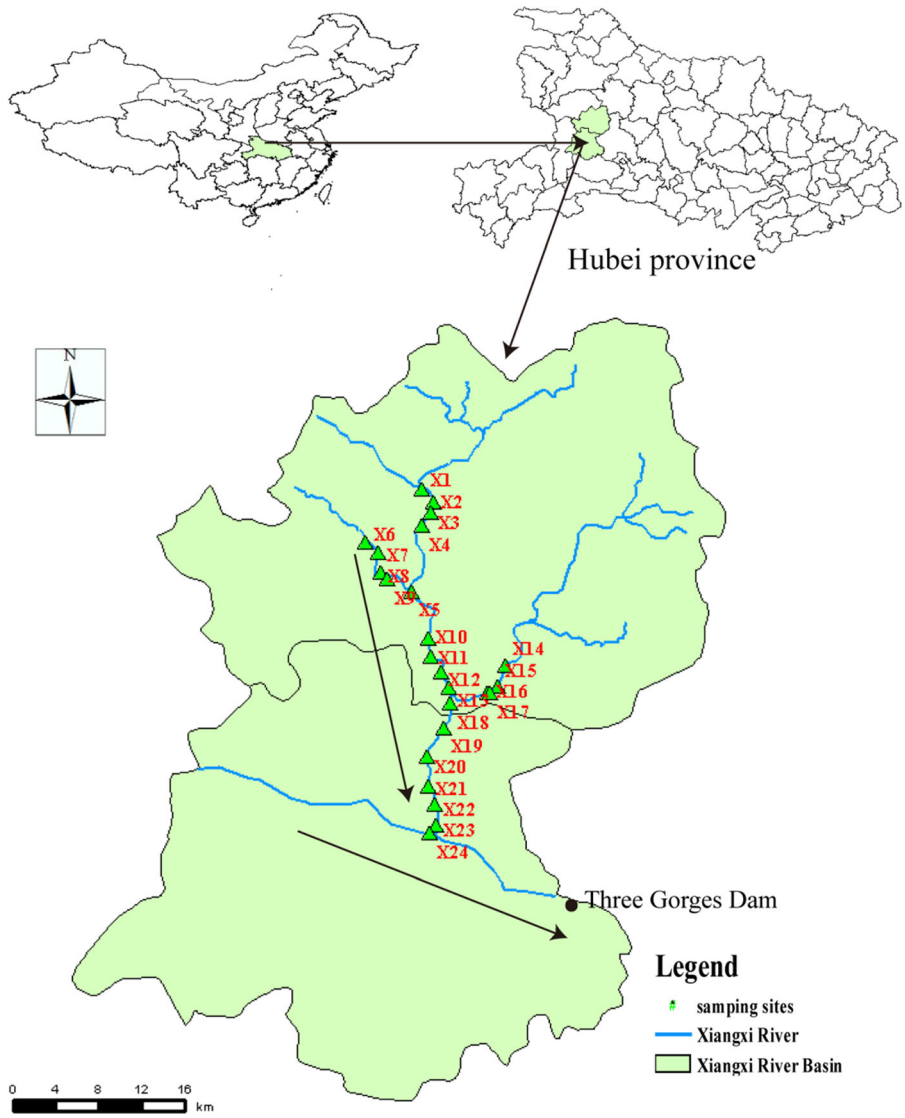

Fig. 1 Study area and the distribution of sampling sites in the Xiangxi River

Sample collection and preparation

Twenty-four samples were collected from upstream to downstream in the Xiangxi River in November 2017. The distribution of sampling sites is shown in Fig. 1. Sampling sites X1–X9 are located upstream of the river. Samples were collected in two upstream tributaries in order to analyze the source of HMs. Sampling sites X1–X4 are located in the Gufu River, a tributary of the Xiangxi River, and sampling sites X6–X9 are located in the Nanyang River, another tributary of the Xiangxi River. Sampling site X5 is located at the confluence of the Gufu and Nanyang rivers. Sampling sites X10–X13 and X18–X23 are located along the main stem of Xiangxi River. Sampling site X24 is located at the intersection of the Xiangxi River and the Yangtze River basin. Sampling sites X14–X17 are located in the Gaolan River, another tributary of the Xiangxi River. A mobile phone equipped with global positioning system (GPS) was used to determine the location of the sampling points, and the location information was recorded in a notebook. Water samples were collected in 1 L polyethylene bottles near the center of the river at a depth of 20 cm. Sample bottles were washed and rinsed with deionized water in the lab and then rinsed with river water on site before collecting the sample. Additionally, water samples were filtered through a 0.45 μm membrane filter acidized with 1% HNO_3. All the samples were transported to the laboratory, stored at − 4 °C, and analyzed in triplicate.

Sample analysis

Metals were determined using ICP-MS (Thermo Xseries II, Germany). This equipment can efficiently and conveniently detect many kinds of HMs simultaneously with low detection limits. The standard curve and recovery rate of standard solutions were used to determine HMs concentrations (Zhang et al. 2018c; Zhong et al. 2018). Prior to sample analyses, the following steps were also taken: (1) calibration of the mass spectrometer according to the manufacturer's instructions; (2) rinsing with HNO_3 until the signal is minimized; (3) addition of internal standard elements (Zhang al. 2018d). If the sample concentration exceeded the calibration curve range, it was diluted with 1% HNO_3 and reanalyzed. The detection limits for As, Hg, Cu, Pb, Cd, Zn, Mn, and Ni are 0.12 μg/L, 0.03 μg/L, 0.08 μg/L, 0.09 μg/L, 0.05 μg/L, 0.67 μg/L, 0.12 μg/L, and 0.06 μg/L, respectively (GB HJ 700-2014).

The quality assurance/quality control (QA/QC) plan included blanks, duplicate samples, and calibration using standard solutions. Blanks were tested after each two samples. Standard recovery rates were all between 89% and 112%. Each sample was analyzed in triplicate ($n = 3$). The deviation of the three duplicate samples was routinely less than 5%, and the correlation coefficient of the calibration curve was ≥ 0.999. The QA/QC results validate the results of HM analysis.

Assessment of heavy metal pollution

The contamination levels of HMs in the Xiangxi River were assessed using the comprehensive pollution index (CPI) (Li et al. 2017a), which is defined as the ratio of the actual concentration of HMs to the national standard. The CPI is calculated by the following equation:

$$\mathrm{CPI} = \frac{1}{m}\sum_{i=1}^{i=m}\frac{C_i}{C_s} \quad (1)$$

where C_i is the actual concentration of the ith HM (mg/L), C_s is the reference value listed in the Environmental Quality Standards for Surface Water (GB3838-2002) (MEP 2002; Zhang et al. 2018a), and m is a constant parameter. Since the Xiangxi River is closely related to human activities and is an important source of irrigation water, C_s values were set according to the Grade III standards within the limits of GB3838-2002, i.e.: As: 0.05 mg/L; Hg: 0.0001 mg/L; Cu: 1 mg/L; Pb: 0.05 mg/L; Cd: 0.005 mg/L; Zn: 1 mg/L; Ni: 0.02 mg/L; Mn: 0.1 mg/L (Zhang et al. 2018a). The level of HMs pollution was ranked from 0–3 based on the CPI classification proposed by Li et al. (2017b), which is summarized in Table S1 of the Supplementary Information.

Potential ecological risk index

The extent of ecological risk posed by HMs at the 24 sampling sites was estimated using the potential ecological risk index (RI). This index combines the HMs concentration with the toxicity of each individual HM to quantify the ecological risks of the HMs present

in water (Ke et al. 2017; Zhang et al. 2018e). The RI is calculated using the following equation:

$$\mathrm{RI} = \sum_{i=1}^{m} E_{\mathrm{r}}^{i} = \sum_{i=0}^{m} T_{\mathrm{r}}^{i} \frac{C^{i}}{C_{n}^{i}} \tag{2}$$

$$E_{\mathrm{r}}^{i} = T_{\mathrm{r}}^{i} C_{\mathrm{f}}^{i} \tag{3}$$

where E_{r}^{i} is the ecological risk of an individual HM (designated as i), and T_{r}^{i} and C_{f}^{i} are the toxic response factor and contamination factor for HM(i); RI is the comprehensive ecological risk of the total HM contamination at a given sampling site, C^{i} is the measured HM concentration at the sampling site and C_{n}^{i} is the reference value of HM(i). T_{r}^{i} for As, Hg, Cu, Pb, Cd, Zn, Mn, and Ni are 10, 40, 5, 5, 30, 1, 1, and 5, respectively (Hakanson 1980; Wang et al. 2018a; Chen et al. 2018).

The ecological risks of individual HMs were divided into the following five levels: (1) low risk ($E_{\mathrm{r}}^{i} < 40$); (2) moderate risk ($40 \leq E_{\mathrm{r}}^{i} < 80$); (3) considerable risk ($80 \leq E_{\mathrm{r}}^{i} < 160$); (4) high risk ($160 \leq E_{\mathrm{r}}^{i} < 320$); and (5) very high risk ($E_{\mathrm{r}}^{i} \geq 320$) (Zhou et al. 2018). Meanwhile, the RI value of HMs was evaluated using the following classification system: low risk ($\mathrm{RI} < 150$); moderate risk ($150 \leq \mathrm{RI} < 300$); high risk ($300 \leq \mathrm{RI} < 600$); and very high risk ($\mathrm{RI} \geq 600$) (Zhang et al. 2018b). The details of these two risk classification systems are presented in Table S2 in the Supplementary Information.

Estimation of risk to human health

In order to estimate the health risk to the local residents caused by exposure to HMs, the human health risk evaluation method proposed by the US Environmental Protection Agency (EPA; EPA 2013) was used. There are three main ways of human exposure to HMs: direct ingestion, inhalation, and skin contact (Zhang et al. 2017b). Considering the large number of residents along both sides of the Xiangxi River who usually wash their clothes in the river, two main exposure pathways—namely skin contact and direct ingestion—were used to evaluate the risk of HMs in water to human health:

$$\mathrm{EDI}_{m} = C_{i} * \frac{\mathrm{IR} * \mathrm{EF} * \mathrm{ED}}{\mathrm{BW} * \mathrm{AT}} \tag{4}$$

$$\mathrm{EDI}_{\mathrm{d}} = C_{i} * \frac{\mathrm{SA} * \mathrm{Kp} * \mathrm{ET} * \mathrm{EF} * \mathrm{ED} * \mathrm{CF}}{\mathrm{BW} * \mathrm{AT}} \tag{5}$$

where $\mathrm{EDI}_{\mathrm{m}}$ represents the average daily HMs intake through ingestion and $\mathrm{EDI}_{\mathrm{d}}$ represents the average daily HMs intake through skin contact. The other evaluated criteria are listed in Table S3.

Additionally, the hazard quotient (HQ) from ingestion (HQ_{m}) and skin contact (HQ_{d}) was used to assess non-carcinogenic risks. The hazard index (HI), which is the sum of HQ_{m} and HQ_{d}, was employed to estimate the total potential non-carcinogenic risk of each HMs:

$$\mathrm{HQ}_{\mathrm{m}} = \frac{\mathrm{EDI}_{\mathrm{m}}}{\mathrm{rfD}_{\mathrm{m}}} \tag{6}$$

$$\mathrm{HQ}_{\mathrm{d}} = \frac{\mathrm{EDI}_{\mathrm{d}}}{\mathrm{rfD}_{\mathrm{d}}} \tag{7}$$

$$\mathrm{rfD}_{\mathrm{d}} = \mathrm{rfD}_{\mathrm{m}} * \mathrm{ABS}_{\mathrm{g}} \tag{8}$$

$$\mathrm{HI} = \mathrm{HQ}_{\mathrm{m}} + \mathrm{HQ}_{\mathrm{d}} \tag{9}$$

where $\mathrm{rfD}_{\mathrm{m}}$ and $\mathrm{rfD}_{\mathrm{d}}$ are the daily reference amount of HMs (μg/kg/day) through ingestion and skin contact, respectively. The values of rfDm and rfDd were obtained from the US EPA (2013), and $\mathrm{ABS}_{\mathrm{g}}$ is dermal absorption factor which is a constant coefficient. There was considered to be little adverse effect on the health of the local residents when the HI is < 1 and potential adverse effects when the HI is ≥ 1.

Statistical analysis

Tracing the source of HMs is valuable for effectively controlling HMs pollution. Previous studies have used principal component analysis (PCA) and Pearson correlation analysis to identify the potential sources of HMs (Islam et al. 2018). Pearson correlation is a correlation analysis method that is used to measure the strength of the correlation between data pertaining to two sets of data. In this study, we used Pearson correlation analysis to determine the correlation between the concentrations of different HMs. The correlations between the concentrations of individual HMs at all sampling sites were analyzed by constructing a Pearson correlation matrix. The results of correlation analysis help to verify the results of factor analysis (Gu and Gao 2018).

Principal component analysis uses dimensional reduction to transform multiple indices into several

Table 1 The mean concentrations of heavy metals (HMs) in the Xiangxi River (this study) and other rivers

River	Mean ± Std. dev. (μg/L)								Reference
	As	Hg	Cu	Pb	Cd	Zn	Mn	Ni	
Xiangxi River, China	0.65 ± 0.46	0.05 ± 0.04	3.21 ± 0.83	10.59 ± 7.33	0.17 ± 0.13	2.4 ± 2.61	12,415.83± 5273.58	6.2 ± 1.66	This study
Wen-Rui Tang River, China	1.71 ± 0.00	0.003 ± 0.00	20.9 ± 2.40	4.23 ± 0.15	0.98 ± 0.05	72.1 ± 6.0	–	–	Qu et al. (2018)
Karnaphuli River, Bangladesh	34.46 + 9.87	–	–	16.83 + 6.17	10.64 + 4.49	–	–	–	Ali et al. (2016)
Yanghe River, China	–	–	21.7	22.00	0.19	96.90	–	–	Kuang et al. (2016)
Han River, China	10.74 ± 1.89	–	7.76 ± 0.46	7.37 ± 1.22	3.21 ± 2.83	–	42.2 ± 22.82	1.15± 0.67	Li and Zhang (2010)

Std. dev. standard deviation

Fig. 2 Kriging interpolation of heavy metal concentrations within the Xiangxi River system

independent comprehensive indices with little loss of information, on the premise of losing little information (Zhang et al. 2018c). The principal components which represent most of the information about the original metric are a linear combination of the original variables (Liu et al. 2018b). The Kaiser–Meyer–Olkin (KMO) value and Bartlett sphericity tests were used to estimate the validity of PCA. To make the extracted principal components more representative, the principal components were extracted after varimax rotation (Cheng et al. 2018). All statistical analyses were performed using the SPSS software (v.20.0; IBM, Armonk, NY, USA).

Results and discussion

Concentrations and spatial distribution of heavy metals in the Xiangxi River

The statistical analysis of HMs concentrations in the Xiangxi River and the other sampled rivers is presented in Table 1. The concentrations of most HMs were low at all sampling sites. The exception was Mn, whose concentration ranged from 570.75 to 2106.73 mg/L. The concentrations of Mn at sampling sites X1, X3, and X4 were more than twice as much as those at sampling sites X18–X23. This may be due to the presence of mining companies upstream of these sampling sites (Li et al. 2014). The order of the mean values of HMs concentrations across all sampling sites was: Mn > Hg > Ni > Pb > Cd > As > Cu > Zn. Compared to other rivers, the concentrations of most HMs ranked at a medium level. The measured concentrations of Cu and Cd were lower than those which have been measured in the Wen-Rui Tang River, China (Qu et al. 2018), and the Karnaphuli River, Bangladesh (Ali et al., 2016), respectively. However, the concentrations of Mn measured in the Xiangxi River in the present study are much higher than those measured in the Han River, China (Li and Zhang 2010). In future studies, the levels of heavy metals in aquatic organisms and sediment can be investigated in order to further assess the HMs contamination of the Xiangxi River.

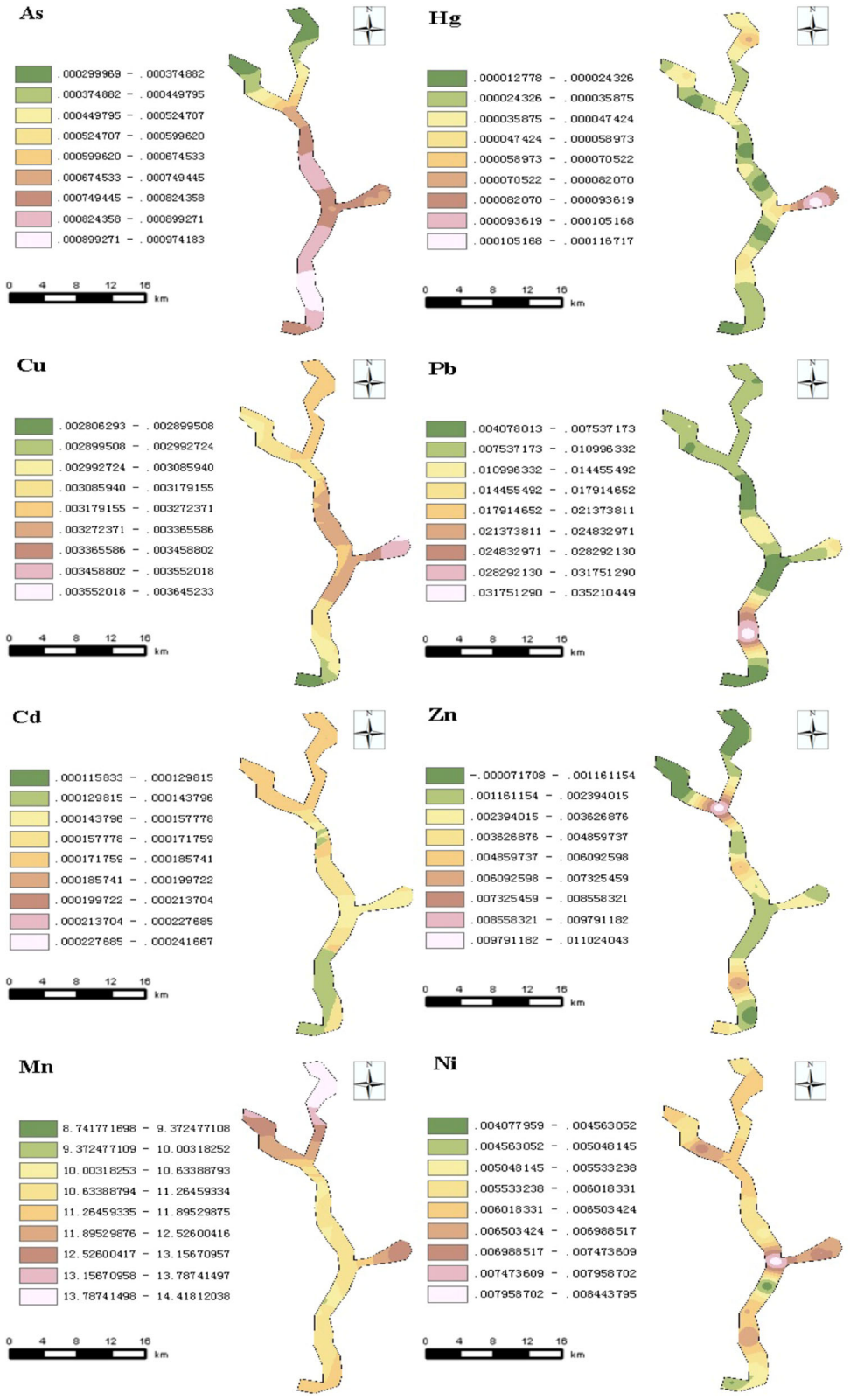
As
.000299969 - .000374882
.000374882 - .000449795
.000449795 - .000524707
.000524707 - .000599620
.000599620 - .000674533
.000674533 - .000749445
.000749445 - .000824358
.000824358 - .000899271
.000899271 - .000974183
0 4 8 12 16 km
Hg
.000012778 - .000024326
.000024326 - .000035875
.000035875 - .000047424
.000047424 - .000058973
.000058973 - .000070522
.000070522 - .000082070
.000082070 - .000093619
.000093619 - .000105168
.000105168 - .000116717
0 4 8 12 16 km
Cu
.002806293 - .002899508
.002899508 - .002992724
.002992724 - .003085940
.003085940 - .003179155
.003179155 - .003272371
.003272371 - .003365586
.003365586 - .003458802
.003458802 - .003552018
.003552018 - .003645233
0 4 8 12 16 km
Pb
.004078013 - .007537173
.007537173 - .010996332
.010996332 - .014455492
.014455492 - .017914652
.017914652 - .021373811
.021373811 - .024832971
.024832971 - .028292130
.028292130 - .031751290
.031751290 - .035210449
0 4 8 12 16 km
Cd
.000115833 - .000129815
.000129815 - .000143796
.000143796 - .000157778
.000157778 - .000171759
.000171759 - .000185741
.000185741 - .000199722
.000199722 - .000213704
.000213704 - .000227685
.000227685 - .000241667
0 4 8 12 16 km
Zn
-.000071708 - .001161154
.001161154 - .002394015
.002394015 - .003626876
.003626876 - .004859737
.004859737 - .006092598
.006092598 - .007325459
.007325459 - .008558321
.008558321 - .009791182
.009791182 - .011024043
0 4 8 12 16 km
Mn
8.741771698 - 9.372477108
9.372477109 - 10.00318252
10.00318253 - 10.63388793
10.63388794 - 11.26459334
11.26459335 - 11.89529875
11.89529876 - 12.52600416
12.52600417 - 13.15670957
13.15670958 - 13.78741497
13.78741498 - 14.41812038
0 4 8 12 16 km
Ni
.004077959 - .004563052
.004563052 - .005048145
.005048145 - .005533238
.005533238 - .006018331
.006018331 - .006503424
.006503424 - .006988517
.006988517 - .007473609
.007473609 - .007958702
.007958702 - .008443795
0 4 8 12 16 km

The spatial distributions of each HM in the Xiangxi River and its tributaries were obtained using the kriging interpolation tool in the ArcGIS software (v.10.2; Esri, Redlands, CA, USA) (Zhang et al. 2018b). The interpolation region was defined as the sampled stream section (i.e., the section covered by sites X1–X24). The results are shown in Fig. 2. As shown in the figure, HMs at low concentrations do not display a well-defined spatial distribution pattern. Moving from the upstream to the downstream area, the concentration of As gradually increases, while the concentration of Mn gradually decreases.

High concentrations of Hg occur in the Nanyang River; however, low concentrations occur in all other locations. Generally, HMs pollution is higher in the upstream reaches than the downstream. The concentrations of Zn and Ni do not appear to have a regular spatial distribution. Additionally, there was no significant difference in the spatial distributions of the concentrations of Cu and Cd from the north to the south of the sampled area. Low concentrations of Cu and Cd were observed at the intersection of the Xiangxi and Yangtze rivers. The concentrations of Pb were high in the central regions and decreased toward the edges of the sampled area. Seasonal HM pollution surveys in the Xiangxi River can be used to observe the influence of periodic impoundment on HM concentrations in the TGR.

Fig. 4 The ecological risk values of different HMs at each sampling sites ▶

Pollution assessment based on the CPI

The results of the assessment of HMs contamination using the CPI method are shown in Fig. 3. Figure 3a shows the CPI results along the Gufu River and down the main stem of the Xiangxi River to the TGR.

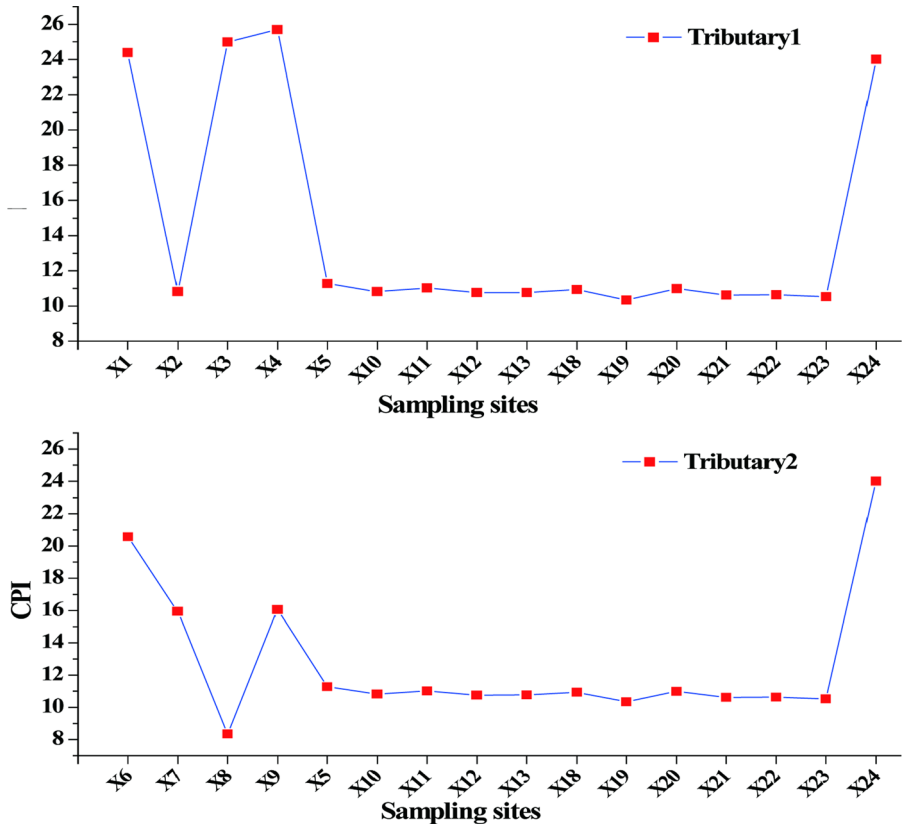

Fig. 3 Variation of the comprehensive pollution index (CPI) with sampling site moving down the Gufu River and the Xiangxi River (**a**) and moving down the Nanyang River and Xiangxi River (**b**)

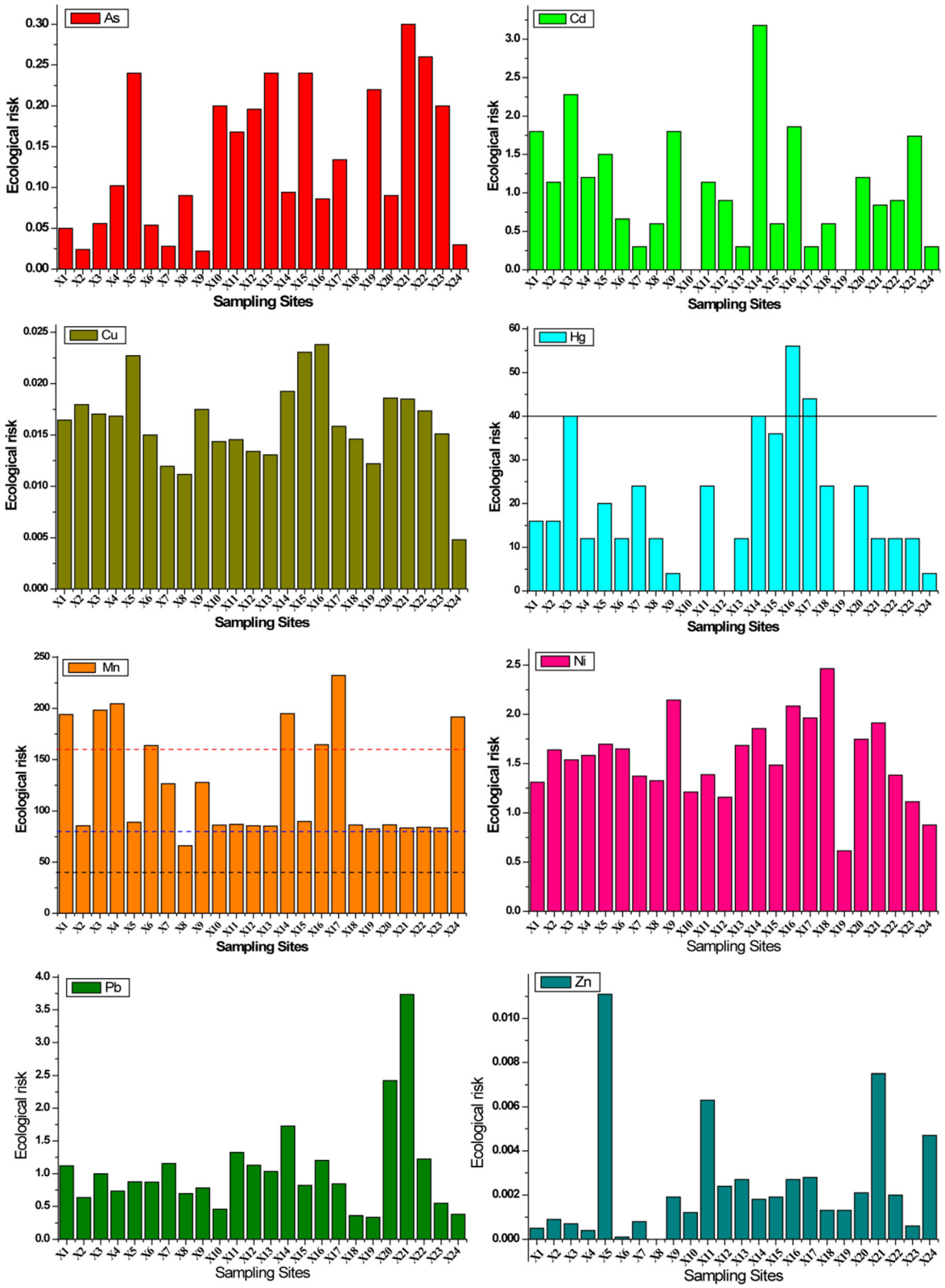
As
Cd
Cu
Hg
Mn
Ni
Pb
Zn
Ecological risk
Sampling Sites
X1 X2 X3 X4 X5 X6 X7 X8 X9 X10 X11 X12 X13 X14 X15 X16 X17 X18 X19 X20 X21 X22 X23 X24

Figure 3b shows the evaluation results along the Nanyang River and down the main stream of the Xiangxi River to the TGR. Sites X5 and X10–X24 are the same sampling points in Fig. 3a, b. As shown in Fig. 3a, the Gufu section is relatively polluted, which may be related to the distribution of upstream mine tailings. Meanwhile, CPI values along the Xiangxi main stem, sites X10–X23, are lower and followed by a spike at site X24. Site X24 is at the Xiangxi River outlet to TGR and reflects the higher pollution levels in Yangtze River. HM pollution in Nanyang River is lower than in Gufu River (Fig. 3b). Additionally, HMs pollution gradually decreases from upstream to downstream due to the deposition of sediment in the upstream region.

Potential ecological risks

Ecological risk (Er) assessment of individual heavy metals

To further evaluate the degree of HMs pollution in the Xiangxi River, the ecological risk (Er) index was used. As shown in Fig. 4, the Er values of most HMs were below the minimum risk value (Er = 40) (Zhou et al. 2018). The Er values of the eight investigated HMs over all sampling sites followed the following order: Mn (2979.8) > Hg (456) > Ni (37.2025) > Pb (25.407) > Cd (25.14) > As (3.124) > Cu (0.38505) > Zn (0.0575).

Despite the fact that the Hg contamination was the lowest of the eight HMs, high Er values of Hg were observed at five sampling sites, namely X6, X14, X15, X16, and X17. It has previously been reported that rural settlements are a major source of Hg pollution (Zhang et al. 2018b). The area around the Xiangxi River is densely populated, with inhabitants principally relying on coal for heating. Due to its high volatility, most Hg is produced as a melt gas during combustion and then transmitted to the soil under the action of deposition (Lv and Liu 2019). Furthermore, the soil which contains Hg was washed into the river by rainwater. Therefore, the content of Hg in the Xiangxi River is strongly positively correlated with coal combustion in the surrounding areas. The Er values of Mn at all sampling sites exceeded the low risk level, and 12 sampling sites reach considerable risk level. According to the classification of Er in Table S2, the potential Er associated with Mn was very high at sampling sites X1, X3, X4, X6, X14, X16, and X17. This result indicates that Mn poses the highest ecological risk index of all of the eight studied HMs. Overall, the assessment of Er indicates that water pollution control measures should be adopted in the Xiangxi River, especially for Mn and Pb.

Comprehensive potential ecological risks of HMs

The calculation results of RI based on Eqs. (2) and (3) are shown in Fig. 5. The RI values of the HMs ranged from 80.82 to 279.56. None of the sampling sites had

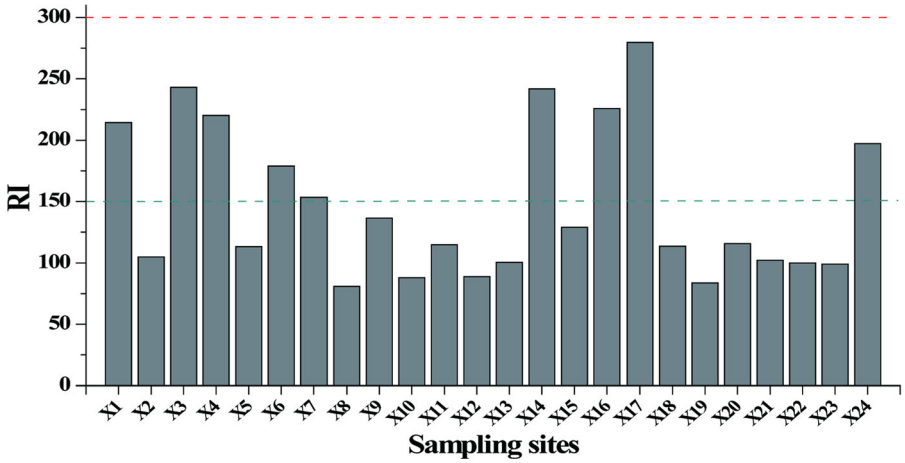

Fig. 5 The assessment results for the potential ecological risk index (RI) across all sampling sites

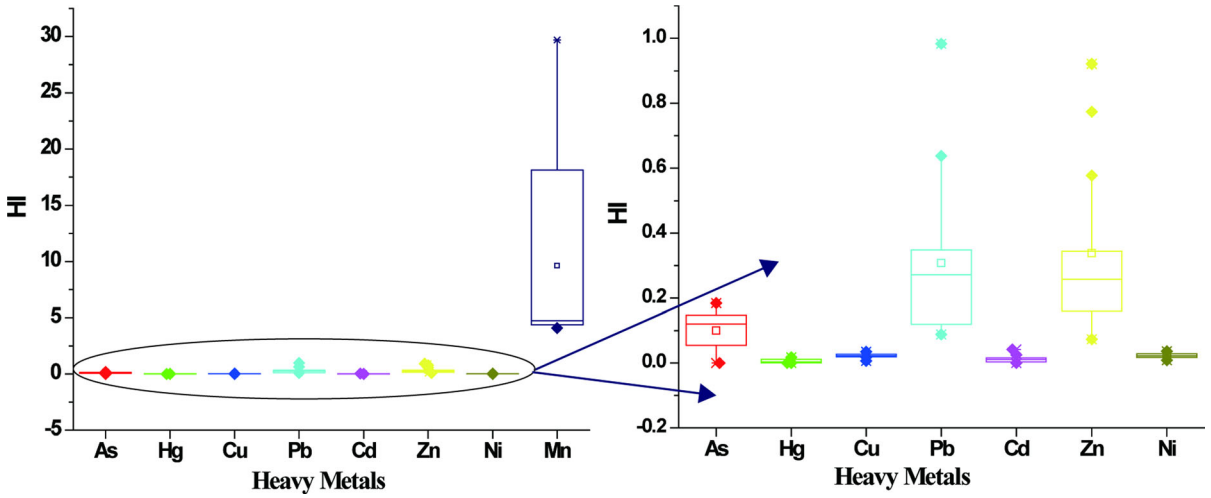

Fig. 6 Health risk assessment (HI) values for each heavy metal, averaged across sampling sites. In the right panel, Mn was omitted and the HI scale expanded to more clearly show the box plots of the remaining heavy metals. HI values < 1 indicate a low risk to health

an RI value of more than 300. For most sampling sites, the calculated RI values are lower than the lowest ecological risk level. As shown in Fig. 5, no sampling sites are at the very high or considerable risk level, while a moderate risk was found at nine sampling sites, and a low risk was found at 15 sampling sites.

There was a clear correlation between the distribution of RI values (Fig. 5) and the distribution of Mn values (Table S2, Supplementary Information). Sampling sites X1, X3, X4, X14, X16, X17, and X24 exhibited relatively high HMs contamination and high ecological risks. Therefore, the results of the HMs pollution assessment based on the CPI are consistent with the results of the RI assessment. Overall, the RI values of the tributaries were higher than those of the main river. Meanwhile, the RI values of the upstream area were generally higher than those of the downstream area. At sampling sites X10–X13, the RI values of HMs were low and the pollution level was low.

In order to analyze the contribution of each of the measured HMs to the total ecological risk at each sampling site, the RI of each HM was converted to a percentage of the total RI. As displayed in Figure S1 (Supplementary Information), Mn represents the main ecological risk at each sampling site, followed by Pb. Therefore, the sources of Mn pollution in the Xiangxi River should be focused on and appropriate countermeasures to such pollution should be implemented.

Human health risk assessment

The non-carcinogenic health risks of HMs to local residents via exposure through different channels are shown in Fig. 6. The results are presented in box plots which can describe the discrete distribution of data in a relatively stable way. As shown in Fig. 6, Mn has the highest HI value of all of the measured HMs.

Since the Xiangxi River provides irrigation water for agriculture, the presence of HMs in the river can lead to the accumulation of HMs in crops and can thereby lead to their accumulation in the human body via crop consumption (Jiang et al. 2016). Thus, ingestion of food and water is the primary exposure pathway. The HI values of the HMs except for Mn were less than 1 at all sampling sites indicating that the human health risk posed by HMs in Xiangxi River is low (Wang et al. 2018b). However, the HI value of Mn exceeded 1, indicating that Mn presents risks to human health.

Analysis of the possible sources of heavy metals

Correlation analysis

The correlation matrix of eight HMs is provided in Table 2. The results showed that Hg, Cu, Ni, and Cd were significantly positive correlated ($p < 0.01$), but they did not correlate with other HMs. The strong correlations between these three metals indicate that

Table 2 Correlation analysis between eight heavy metals

	As	Hg	Cu	Pb	Cd	Zn	Mn	Ni
As	1							
Hg	− 0.191	1						
Cu	0.226	**0.566****	1					
Pb	0.309	0.170	0.333	1				
Cd	− 0.229	**0.440***	**0.517****	0.235	1			
Zn	**0.457***	0.032	0.225	0.374	0.014	1		
Mn	− **0.471***	**0.432***	− 0.008	− 0.087	0.349	− 0.180	1	
Ni	-.269	**0.517****	**0.536****	0.294	0.321	0.119	0.149	1

Significant correlations are in boldface

*Significant correlation at $p < 0.05$; ** significant correlation at $p < 0.01$

they may come from a common source (Li et al. 2018). However, these three metals showed no significant correlations with any other metals. Additionally, Mn exhibited positive correlations with Hg and As ($p < 0.05$), which similarly suggests that these three HMs may emanate from a common source. However, these three metals showed no significant correlation with any other metals. Cd is widespread in agricultural materials (Lv and Liu 2019), and thus, the detected Hg and Ni may also mainly emanate from agricultural sources.

The correlations shown in Table 2 can be used to estimate the sources of HMs (Ma et al. 2016). For example, the fact that As is negatively correlated with Mn and Hg, but Mn and Hg are positively correlated with each other indicates that As comes from one source and Mn and Hg come from another (Wang et al. 2015).

Principal component analysis

Principal component analysis was used to further confirm major sources of pollution in the study area (Liu et al. 2018c). Table 3 shows the results of PCA before and after rotation, with the latter better reflecting empirical realities. The rotation method of variance maximization was adopted to select factors with eigenvalues greater than 1.

The KMO value (0.561) and Bartlett's test value (< 0.001) prove that the PCA results are reliable (Ma et al. 2018). Figure S2 shows the eigenvalues of all the components. The eigenvalues of components 1 and 2 are greater than 1 and together explain nearly 70% of the total variance. Thus, components 1 and 2 were extracted as the main components.

The first principal component (PC1) explained 34.64% of the total variance. PC1 was related to Hg (0.817), Cu (0.763), Ni (0.749), and Cd (0.732). This result is consistent with the results of the foregoing Pearson's correlation analysis. PC1 probably reflects agricultural activities since agriculture is the main industry in the Xiangxi River basin (Chai et al. 2017; Hubei Statistical Yearbook 2017).

Agricultural activity has previously been reported as a source of Cu pollution (Marrugo-Negrete et al. 2017). Specifically, the accumulation of Cu in soil may be caused by the excessive application of pesticides, herbicides, or fertilizers in cropland (Elumalai et al. 2017; Zhang et al. 2016). Furthermore, HMs from various sources (transportation, industrial, and human activities) can be washed into rivers by storm runoff. Moreover, HMs in the reservoir bank and the hydro-fluctuation belt can migrate into river water. When the external conditions (i.e., redox, pH) are appropriate, HMs in sediments will be released into water and thus cause HMs pollution (Gao et al. 2018a). Therefore, it is imperative to take engineering measures to control HMs pollution in bank soil, for example ecological restoration by planting, the reduction of peripheral industries, and the conversion of farmland to forest.

The second principal component explained 26.36% of the total variance. This component was related to As (0.838) and Zn (0.716). This is also consistent with the results of the Pearson correlation analysis, in which Zn was positively correlated with As. The second

Table 3 Component matrices for the HMs

Metal	Component matrix		Rotated component matrix	
	PC1	PC2	PC1	PC2
As	− 0.188	0.845	− 0.217	**0.838**
Hg	0.813	− 0.153	**0.817**	− 0.126
Cu	0.775	0.353	**0.763**	0.379
Pb	0.427	0.578	0.408	0.592
Cd	0.728	− 0.136	**0.732**	− 0.111
Zn	0.169	0.710	0.145	**0.716**
Mn	0.413	− 0.624	0.434	− 0.610
Ni	0.750	0.000	**0.749**	0.026

PC1: first principal component. PC2: second principal component

principal component could plausibly be from transportation and upstream mining activities (Cai et al. 2018; Men et al. 2018). Mining and smelting produce large quantities of pollutants, such as fine-grained mineral ores, alkaline As residues, and ore weathering products (Wang et al. 2011). Chen and Lu (2018) collected 193 samples of river water from Xian, China, and used EPA positive matrix factorization (PMF) software to identify HM sources. Their results showed that Zn was related to traffic emissions.

By-products of mining activities may be discharged into surrounding river channels and thereby result in excessive HMs concentrations in water and sediments. With the action of surface runoff, HMs in the topsoil around mining areas may be transported into rivers, which increases the concentration of HMs in the water (Zhang et al. 2018e). To further identify the sources of heavy metals, future studies can consider local geomorphological characteristics, population density, and data from statistical yearbooks.

Conclusions

In this study, samples were collected from 24 sites in the Xiangxi River system and analyzed for eight HMs. The results were used to assess HM contamination of Xiangxi River, the ecological risk and public health threat posed by the HMs, and identify sources of pollution. This was the first investigation of HMs in the Xiangxi River, and the primary findings are as follows: (1) The concentrations of Mn were high, whereas those of the other seven metals were low. HM levels in Xiangxi River were generally mid-range compared to other rivers. (2) Comparison of the CPI by site indicated that HM pollution is heavier in the upper reaches of the study area. The spatial distribution of HM concentrations within the river system supports this conclusion. (3) Mn and Pb were the primary contributors to ecological risk posed by HMs. (4) The HI indicates that only Mn poses a threat to the health of local residents and Mn mitigation should be given special attention. (5) HM pollution in Xiangxi River arises primarily from agriculture and upstream mining, with contributions from coal combustion and transportation. The results of this study provide a reference that will support prioritization and planning for HM pollution control in the Xiangxi River region.

Acknowledgements This work was supported by the Hubei Province Innovation Group Project (No: 2015CFA021), the Open Research Program of the Engineering Research Center of Eco-environment in Three Gorges Reservoir Region of the Ministry of Education (No: KF2018-03), the Research Fund for Excellent Dissertation of the China Three Gorges University (2020BSPY015), and the National Key Research and Development Program of China (No: 2016YFD0800904).

References

Ali, M. M., Ali, M. L., Islam, M. S., & Rahman, M. Z. (2016). Preliminary assessment of heavy metals in water and sediment of Karnaphuli River, Bangladesh. *Environmental Nanotechnology, Monitoring & Management, 5,* 27–35. https://doi.org/10.1016/j.enmm.2016.01.002.

Bai, J., Zhao, Q., Wang, W., Wang, X., Jia, J., Cui, B., et al. (2019). Arsenic and heavy metals pollution along a salinity gradient in drained coastal wetland soils: Depth

distributions, sources and toxic risks. *Ecological Indicators, 96,* 91–98. https://doi.org/10.1016/j.ecolind.2018.08.026.

Cai, L. M., Wang, Q. S., Luo, J., Chen, L. G., Zhu, R. L., Wang, S., et al. (2018). Heavy metals contamination and health risk assessment for children near a large Cu-smelter in central China. *Science of the Total Environment, 650,* 725–733. https://doi.org/10.1016/j.scitotenv.2018.09.081.

Chai, L., Li, H., Yang, Z., Min, X., Liao, Q., Liu, Y., et al. (2017). Heavy metals and metalloids in the surface sediments of the Xiangjiang River, Hunan, China: Distribution, contamination, and ecological risk assessment. *Environmental Science and Pollution Research, 24*(1), 874–885. https://doi.org/10.1007/s11356-016-7872-x.

Chen, Y., Jiang, X., Wang, Y., & Zhuang, D. (2018). Spatial characteristics of heavy metals pollution and the potential ecological risk of a typical mining area: A case study in China. *Process Safety and Environmental Protection, 113,* 204–219. https://doi.org/10.1016/j.psep.2017.10.008.

Chen, X., & Lu, X. (2018). Contamination characteristics and source apportionment of heavy metals in topsoil from an area in Xi'an city, China. *Ecotoxicology and Environmental Safety, 151,* 153–160. https://doi.org/10.1016/j.ecoenv.2018.01.010.

Cheng, Z., Chen, L. J., Li, H. H., Lin, J. Q., Yang, Z. B., Yang, Y. X., et al. (2018). Characteristics and health risk assessment of heavy metals exposure via household dust from urban area in Chengdu, China. *Science of the Total Environment, 619–620,* 621–629. https://doi.org/10.1016/j.scitotenv.2017.11.144.

Chuo, M., Ma, J., Liu, D., & Yang, Z. (2019). Effects of the impounding process during the flood season on algal blooms in Xiangxi Bay in the Three Gorges Reservoir, China. *Ecological Modelling, 392,* 236–249. https://doi.org/10.1016/j.ecolmodel.2018.11.017.

Elumalai, V., Brindha, K., & Elango, L. (2017). Regional and temporal variation in minor ions in groundwater of a part of a large river delta, southern India. *Environmental Monitoring and Assessment, 189*(7), 305.

Gao, Q., He, G., Fang, H., Bai, S., & Huang, L. (2018a). Numerical simulation of water age and its potential effects on the water quality in Xiangxi Bay of Three Gorges Reservoir. *Journal of Hydrology, 566,* 484–499. https://doi.org/10.1016/j.jhydrol.2018.09.033.

Gao, Q., Li, Y., Cheng, Q., Yu, M., Hu, B., Wang, Z., et al. (2016). Analysis and assessment of the nutrients, biochemical indexes and heavy metals in the Three Gorges Reservoir, China, from 2008 to 2013. *Water Research, 92,* 262–274. https://doi.org/10.1016/j.watres.2015.12.055.

Gao, L., Wang, Z., Li, S., & Chen, J. (2018b). Bioavailability and toxicity of trace metals (Cd, Cr, Cu, Ni, and Zn) in sediment cores from the Shima River, South China. *Chemosphere, 192,* 31–42. https://doi.org/10.1016/j.chemosphere.2017.10.110.

Gu, Y. G., & Gao, Y. P. (2018). Bioaccessibilities and health implications of heavy metals in exposed-lawn soils from 28 urban parks in the megacity Guangzhou inferred from an in vitro physiologically-based extraction test. *Ecotoxicology and Environmental Safety, 148,* 747–753. https://doi.org/10.1016/j.ecoenv.2017.11.039.

Hakanson, L. (1980). An ecological risk index for aquatic pollution control: A sedimentological approach. *Water Research, 14*(8), 975–1001.

Huang, Y., Fu, C., Li, Z., Fang, F., Ouyang, W., & Guo, J. (2019). Effect of dissolved organic matters on adsorption and desorption behavior of heavy metals in a water-level-fluctuation zone of the Three Gorges Reservoir, China. *Ecotoxicology and Environmental Safety, 185,* 109695. https://doi.org/10.1016/j.ecoenv.2019.109695.

Hubei Statistical Yearbook. (2017). *Hubei Provincial Bureau of Statistics, 2017.*

Islam, M. S., Hossain, M. B., Matin, A., & Islam Sarker, M. S. (2018). Assessment of heavy metals pollution, distribution and source apportionment in the sediment from Feni River estuary, Bangladesh. *Chemosphere, 202,* 25–32. https://doi.org/10.1016/j.chemosphere.2018.03.077.

Jiang, L. G., Liang, B., Xue, Q., & Yin, C. W. (2016). Characterization of phosphorus leaching from phosphate waste rock in the Xiangxi River watershed, Three Gorges Reservoir, China. *Chemosphere, 150,* 130–138. https://doi.org/10.1016/j.chemosphere.2016.02.008.

Ke, X., Gui, S., Huang, H., Zhang, H., Wang, C., & Guo, W. (2017). Ecological risk assessment and source identification for heavy metals in surface sediment from the Liaohe River protected area, China. *Chemosphere, 175,* 473–481. https://doi.org/10.1016/j.chemosphere.2017.02.029.

Kuang, C., Shan, Y., Gu, J., Shao, H., Zhang, W., Zhang, Y., et al. (2016). Assessment of heavy metals contamination in water body and riverbed sediments of the Yanghe River in the Bohai Sea, China. *Environmental Earth Sciences, 75*(14), 15–20. https://doi.org/10.1007/s12665-016-5902-0.

Lazo, P., Steinnes, E., Qarri, F., Allajbeu, S., Kane, S., Stafilov, T., et al. (2018). Origin and spatial distribution of metals in moss samples in Albania: A hotspot of heavy metals contamination in Europe. *Chemosphere, 190,* 337–349. https://doi.org/10.1016/j.chemosphere.2017.09.132.

Li, J., Jin, Z., & Yang, W. (2014). Numerical modeling of the Xiangxi River algal bloom and sediment-related process in China. *Ecological Informatics, 22,* 23–35. https://doi.org/10.1016/j.ecoinf.2014.03.002.

Li, X., Li, Z., Lin, C. J., Bi, X., Liu, J., Feng, X., et al. (2018). Health risks of heavy metals exposure through vegetable consumption near a large-scale Pb/Zn smelter in central China. *Ecotoxicology and Environmental Safety, 161,* 99–110. https://doi.org/10.1016/j.ecoenv.2018.05.080.

Li, S., & Zhang, Q. (2010). Risk assessment and seasonal variations of dissolved trace elements and heavy metals in the Upper Han River, China. *Journal of Hazardous Materials, 181*(1–3), 1051–1058. https://doi.org/10.1016/j.jhazmat.2010.05.120.

Li, S., Zhang, J., Guo, E., Zhang, F., Ma, Q., & Mu, G. (2017a). Dynamics and ecological risk assessment of chromophoric dissolved organic matter in the Yinma River Watershed: Rivers, reservoirs, and urban waters. *Environmental Research, 158,* 245–254. https://doi.org/10.1016/j.envres.2017.06.020.

Li, S., Zhang, J., Mu, G., Ju, H., Wang, R., Li, D., et al. (2017b). Spatiotemporal characterization of chromophoric dissolved organic matter (CDOM) and CDOM–DOC

relationships for highly polluted rivers. *Water, 8*(9), 399. https://doi.org/10.3390/w8090399.

Lin, L., Dong, L., Meng, X., Li, Q., Huang, Z., Li, C., et al. (2018). Distribution and sources of polycyclic aromatic hydrocarbons and phthalic acid esters in water and surface sediment from the Three Gorges Reservoir. *Journal of Environmental Sciences, 69,* 271–280. https://doi.org/10.1016/j.jes.2017.11.004.

Lin, L., Li, C., Yang, W., Zhao, L., Liu, M., Li, Q., et al. (2020). Spatial variations and periodic changes in heavy metals in surface water and sediments of the Three Gorges Reservoir, China. *Chemosphere, 240,* 124837. https://doi.org/10.1016/j.chemosphere.2019.124837.

Liu, R., Bao, K., Yao, S., Yang, F., & Wang, X. (2018a). Ecological risk assessment and distribution of potentially harmful trace elements in lake sediments of Songnen Plain, NE China. *Ecotoxicology and Environmental Safety, 163,* 117–124. https://doi.org/10.1016/j.ecoenv.2018.07.037.

Liu, Q., Liao, Y., & Shou, L. (2018b). Concentration and potential health risk of heavy metals in seafoods collected from Sanmen Bay and its adjacent areas, China. *Marine Pollution Bulletin, 131,* 356–364. https://doi.org/10.1016/j.marpolbul.2018.04.041.

Liu, J., Liu, Y. J., Liu, Y., Liu, Z., & Zhang, A. N. (2018c). Quantitative contributions of the major sources of heavy metals in soils to ecosystem and human health risks: A case study of Yulin, China. *Ecotoxicology and Environmental Safety, 164,* 261–269. https://doi.org/10.1016/j.ecoenv.2018.08.030.

Liu, R., Wang, Q., Xu, F., Men, C., & Guo, L. (2017). Impacts of manure application on SWAT model outputs in the Xiangxi River watershed. *Journal of Hydrology, 555,* 479–488. https://doi.org/10.1016/j.jhydrol.2017.10.044.

Luo, M., Chen, Z., Yin, D., Jakada, H., Huang, H., Zhou, H., et al. (2016). Surface flood and underground flood in Xiangxi River Karst Basin: Characteristics, models, and comparisons. *Journal of Earth Science, 27*(1), 15–21. https://doi.org/10.1007/s12583-016-0624-5.

Lv, J., & Liu, Y. (2019). An integrated approach to identify quantitative sources and hazardous areas of heavy metals in soils. *Science of the Total Environment, 646,* 19–28. https://doi.org/10.1016/j.scitotenv.2018.07.257.

Ma, W., Tai, L., Qiao, Z., Zhong, L., Wang, Z., Fu, K., et al. (2018). Contamination source apportionment and health risk assessment of heavy metals in soil around municipal solid waste incinerator: A case study in North China. *Science of the Total Environment, 631–632,* 348–357. https://doi.org/10.1016/j.scitotenv.2018.03.011.

Ma, L., Yang, Z., Li, L., & Wang, L. (2016). Source identification and risk assessment of heavy metals contaminations in urban soils of Changsha, a mine-impacted city in Southern China. *Environment Science and Pollution Resaerch, 23*(17), 17058–17066. https://doi.org/10.1007/s11356-016-6890-z.

Marrugo-Negrete, J., Pinedo-Hernandez, J., & Diez, S. (2017). Assessment of heavy metals pollution, spatial distribution and origin in agricultural soils along the Sinu River Basin, Colombia. *Environment Research, 154,* 380–388. https://doi.org/10.1016/j.envres.2017.01.021.

Men, C., Liu, R., Xu, F., Wang, Q., Guo, L., & Shen, Z. (2018). Pollution characteristics, risk assessment, and source apportionment of heavy metals in road dust in Beijing, China. *Science of the Total Environment, 612,* 138–147. https://doi.org/10.1016/j.scitotenv.2017.08.123.

MEP. (2002). *Environmental quality standards for surface water*. Ministry of Environmental Protection of the People's Republic of China (MEP).

Qu, L., Huang, H., Xia, F., Liu, Y., Dahlgren, R. A., Zhang, M., et al. (2018). Risk analysis of heavy metals concentration in surface waters across the rural-urban interface of the Wen-Rui Tang River, China. *Environmental Pollution, 237,* 639–649. https://doi.org/10.1016/j.envpol.2018.02.020.

Rehman, I. U., Ishaq, M., Ali, L., Khan, S., Ahmad, I., Din, I. U., et al. (2018). Enrichment, spatial distribution of potential ecological and human health risk assessment via toxic metals in soil and surface water ingestion in the vicinity of Sewakht mines, district Chitral, Northern Pakistan. *Ecotoxicology and Environmental Safety, 154,* 127–136. https://doi.org/10.1016/j.ecoenv.2018.02.033.

USEPA (United States Environmental Protection Agency). (2013). *Regional screening level (RSL) summary table*.

Wang, X., He, M., Xi, J., & Lu, X. (2011). Antimony distribution and mobility in rivers around the world's largest antimony mine of Xikuangshan, Hunan Province, China. *Microchemical Journal, 97*(1), 4–11. https://doi.org/10.1016/j.microc.2010.05.011.

Wang, L., Luo, Y., & Dai, Z. (2017). Characteristics and ecological risk assessment of heavy metals in sediments of the Xiangxi River. *Journal of Agro-Environment Science, 36*(8), 1610–1617.

Wang, H., Wu, Q., Hu, W., Huang, B., Dong, L., & Liu, G. (2018a). Using multi-medium factors analysis to assess heavy metals health risks along the Yangtze River in Nanjing, Southeast China. *Environmental Pollution, 243,* 1047–1056. https://doi.org/10.1016/j.envpol.2018.09.036.

Wang, Y., Yang, L., Kong, L., Liu, E., Wang, L., & Zhu, J. (2015). Spatial distribution, ecological risk assessment and source identification for heavy metals in surface sediments from Dongping Lake, Shandong, East China. *CATENA, 125,* 200–205. https://doi.org/10.1016/j.catena.2014.10.023.

Wang, X., Zhang, L., Zhao, Z., & Cai, Y. (2018b). Heavy metals pollution in reservoirs in the hilly area of southern China: Distribution, source apportionment and health risk assessment. *Science of the Total Environment, 634,* 158–169. https://doi.org/10.1016/j.scitotenv.2018.03.340.

Wu, Y., Wang, X., Zhou, J., Bing, H., Sun, H., & Wang, J. (2016). The fate of phosphorus in sediments after the full operation of the Three Gorges Reservoir, China. *Environmental Pollution, 214,* 282–289. https://doi.org/10.1016/j.envpol.2016.04.029.

Xu, T., Wang, F., Guo, Q., Nie, X., Huang, Y., & Chen, (2014). Transfer characteristic and source identification of soil heavy metals from water-level-fluctuating zone along xiangxi river, three-gorges reservoir area. *Environmental Science, 35*(4), 1502–1508.

Yan, H., Huang, Y., Wang, G., Zhang, X., Shang, M., Feng, L., et al. (2016). Water eutrophication evaluation based on rough set and petri nets: a case study in Xiangxi-River, Three Gorges Reservoir. *Ecological Indicators, 69,* 463–472. https://doi.org/10.1016/j.ecolind.2016.05.010.

Zhang, G., Bai, J., Xiao, R., Zhao, Q., Jia, J., Cui, B., et al. (2017a). Heavy metals fractions and ecological risk assessment in sediments from urban, rural and reclamation-affected rivers of the Pearl River Estuary, China. *Chemosphere, 184,* 278–288. https://doi.org/10.1016/j.chemosphere.2017.05.155.

Zhang, Y., Chu, C., Li, T., Xu, S., Liu, L., & Ju, M. (2017b). A water quality management strategy for regionally protected water through health risk assessment and spatial distribution of heavy metals pollution in 3 marine reserves. *Science of the Total Environment, 599–600,* 721–731. https://doi.org/10.1016/j.scitotenv.2017.04.232.

Zhang, Z., Juying, L., Mamat, Z., & QingFu, Y. (2016). Sources identification and pollution evaluation of heavy metals in the surface sediments of Bortala River, Northwest China. *Ecotoxicology and Environmental Safety, 126,* 94–101. https://doi.org/10.1016/j.ecoenv.2015.12.025.

Zhang, Z., Lu, Y., Li, H., Tu, Y., Liu, B., & Yang, Z. (2018a). Assessment of heavy metals contamination, distribution and source identification in the sediments from the Zijiang River, China. *Science of the Total Environment, 645,* 235–243. https://doi.org/10.1016/j.scitotenv.2018.07.026.

Zhang, P., Qin, C., Hong, X., Kang, G., Qin, M., Yang, D., et al. (2018b). Risk assessment and source analysis of soil heavy metals pollution from lower reaches of Yellow River irrigation in China. *Science of the Total Environment, 633,* 1136–1147. https://doi.org/10.1016/j.scitotenv.2018.03.228.

Zhang, X., Wei, S., Sun, Q., Wadood, S. A., & Guo, B. (2018c). Source identification and spatial distribution of arsenic and heavy metals in agricultural soil around Hunan industrial estate by positive matrix factorization model, principle components analysis and geo statistical analysis. *Ecotoxicology and Environmental Safety, 159,* 354–362. https://doi.org/10.1016/j.ecoenv.2018.04.072.

Zhang, T., Xu, W., Lin, X., Yan, H., Ma, M., & He, Z. (2019). Assessment of heavy metals pollution of soybean grains in North Anhui of China. *Science of the Total Environment, 646,* 914–922. https://doi.org/10.1016/j.scitotenv.2018.07.335.

Zhang, Y., Yin, C., Cao, S., Cheng, L., Wu, G., & Guo, J. (2018d). Heavy metals accumulation and health risk assessment in soil-wheat system under different nitrogen levels. *Science of the Total Environment, 622–623,* 1499–1508. https://doi.org/10.1016/j.scitotenv.2017.09.317.

Zhang, L., Zhao, B., Xu, G., & Guan, Y. (2018e). Characterizing fluvial heavy metals pollutions under different rainfall conditions: Implication for aquatic environment protection. *Science of the Total Environment, 635,* 1495–1506. https://doi.org/10.1016/j.scitotenv.2018.04.211.

Zhao, X. J., Gao, B., Xu, D. Y., Gao, L., & Yin, S. H. (2017). Heavy metal pollution in sediments of the largest reservoir (Three Gorges Reservoir) in China: A review. *Environment Science and Pollution Research, 24*(26), 20844–20858. https://doi.org/10.1007/s11356-017-9874-8.

Zhong, W., Zhang, Y., Wu, Z., Yang, R., Chen, X., Yang, J., et al. (2018). Health risk assessment of HMs in freshwater fish in the central and eastern North China. *Ecotoxicology and Environmental Safety, 157,* 343–349. https://doi.org/10.1016/j.ecoenv.2018.03.048.

Zhou, Y., Aamir, M., Liu, K., Yang, F., & Liu, W. (2018). Status of mercury accumulation in agricultural soil across China: Spatial distribution, temporal trend, influencing factor and risk assessment. *Environment Pollution, 240,* 116–124. https://doi.org/10.1016/j.envpol.2018.03.086.

Zhu, H., Bing, H., Wu, Y., Zhou, J., Sun, H., Wang, J., et al. (2019). The spatial and vertical distribution of heavy metal contamination in sediments of the Three Gorges Reservoir determined by anti-seasonal flow regulation. *Science of the Total Environment, 664,* 79–88. https://doi.org/10.1016/j.scitotenv.2019.02.016.

Zhuang, Q., Li, G., & Liu, Z. (2018). Distribution, source and pollution level of heavy metals in river sediments from South China. *CATENA, 170,* 386–396. https://doi.org/10.1016/j.catena.2018.06.037.